

## Dynamics below the Depinning Threshold in Disordered Elastic Systems

Alejandro B. Kolton,<sup>1</sup> Alberto Rosso,<sup>2</sup> Thierry Giamarchi,<sup>1</sup> and Werner Krauth<sup>3</sup>

<sup>1</sup>DPMC-MaNEP University of Geneva, 24 Quai Ernest Ansermet, 1211 Geneva 4, Switzerland

<sup>2</sup>LPTMS, CNRS and Université de Paris-Sud, UMR 8626, Orsay Cedex, 91405, France

<sup>3</sup>CNRS-Laboratoire de Physique Statistique, Ecole Normale Supérieure, 24 rue Lhomond, 75231 Paris Cedex 05, France

(Received 13 March 2006; published 1 August 2006)

We study the steady-state low-temperature dynamics of an elastic line in a disordered medium below the depinning threshold. Analogously to the equilibrium dynamics, in the limit  $T \rightarrow 0$ , the steady state is dominated by a single configuration which is occupied with probability 1. We develop an exact algorithm to target this dominant configuration and to analyze its geometrical properties as a function of the driving force. The roughness exponent of the line at large scales is identical to the one at depinning. No length scale diverges in the steady-state regime as the depinning threshold is approached from below. We do find a divergent length, but it is associated only with the transient relaxation between metastable states.

DOI: 10.1103/PhysRevLett.97.057001

PACS numbers: 74.25.Qt, 05.70.Ln, 64.60.Ht, 75.60.Ch

The physics of elastic systems in disordered media has been the focus of intense theoretical and experimental studies. A continuing challenge has been to understand their response to an applied external force  $f$ . Such a situation is relevant for a large number of experimental driven systems ranging from periodic ones, such as vortex lattices [1] and charge density waves [2], to interfaces, such as domain walls in magnetic [3,4] or ferroelectric [5,6] materials, contact lines [7], and crack propagation [8].

A crucial feature of the zero-temperature motion of these systems is the existence of a threshold force  $f_c$  below which the system is pinned. For  $f > f_c$  the system undergoes a depinning transition [9–13] and moves with a non-zero average velocity. Fisher first viewed the depinning transition as a critical phenomenon [14]. A key idea is that the slow motion close to  $f_c$  proceeds by avalanches of size  $\xi$ , which diverge as  $f_c$  is approached. Indeed, theoretical and numerical works at zero temperature have shown that for  $f \rightarrow f_c^+$ , the correlation length diverges as  $\xi \sim (f - f_c)^{-\nu_{\text{dep}}}$ . The exponent  $\nu_{\text{dep}}$  is related to the roughness exponent  $\zeta_{\text{dep}}$  of the system pinned at  $f_c$ , via the scaling relation  $\nu_{\text{dep}} = 1/(2 - \zeta_{\text{dep}})$ . The length scale  $\xi$  identifies both the typical size of avalanches and the crossover in the roughness behavior [13]. For length scales below  $\xi$ , the roughness is described by the exponent  $\zeta_{\text{dep}}$ , while for scales larger than  $\xi$ , the velocity introduces a time dependent noise. In this regime, for interfaces, quenched disorder becomes equivalent to an effective temperature, and the roughness exponent is equal to the thermal one. The interpretation of depinning as a critical phenomenon suggests that a similar diverging length scale would also exist below  $f_c$ . Indeed, in standard critical phenomena, for length scales smaller than the correlation length the system is critical and crosses over beyond this correlation length to the broken symmetry phase on one side of the transition and to the symmetric phase on the other side. An important question is thus whether an equivalent length is observable in the limit  $f \rightarrow f_c^-$ .

Answering such a question is not an easy task since below  $f_c$  the steady-state velocity vanishes in the long-time limit at zero temperature. This makes methods such as molecular dynamics simulations ill suited. Some authors [15–17] have therefore studied the relaxation of a given initial configuration towards a final zero-velocity state. This analysis allows us to identify a dynamical scaling characterized by a single correlation length diverging with an exponent  $\nu_{\text{dep}}$  as  $f_c$  is approached. However, it has remained unclear how such  $T = 0$  transients relate to the steady-state motion in the large time limit at small but finite temperatures. Below  $f_c$ , it is thus preferable to keep the temperature finite, but direct Langevin dynamics simulations are powerless to clarify whether the limit  $f \rightarrow f_c^-$  is also characterized by a divergent length scale. An analytical tool for addressing this issue is the functional renormalization group (FRG). This method allows one to study, at finite temperature, the slow creep motion [18–21] taking place for  $f \ll f_c$ . In the creep regime, scaling arguments rely on the physical properties of the system at equilibrium ( $f = 0$ ). This phenomenological approach suggests that, for  $f \ll f_c$ , the macroscopic forward motion is produced by activated jumps with typical size  $\xi_T \sim f^{-\nu_{\text{eq}}}$ . The exponent  $\nu_{\text{eq}}$  can be related to the roughness by the same scaling relation,  $\nu_{\text{eq}} = 1/(2 - \zeta_{\text{eq}})$ , but with  $\zeta_{\text{eq}}$  the equilibrium roughness exponent. The FRG analysis [20] shows that  $\xi_T$  plays the role of crossover length between two roughness regimes: on length scales below  $\xi_T$ , the roughness is described by the exponent  $\zeta_{\text{eq}}$ , while for scales larger than  $\xi_T$  it is described by the exponent  $\zeta_{\text{dep}}$ . This regime crosses over, for interfaces, to a pure thermal-like behavior at very large length scales due to the finiteness of the velocity for any nonzero temperature. This FRG finding is thus at variance with the interpretation of the depinning transition as a standard critical phenomenon, since it shows that the roughness  $\zeta_{\text{dep}}$  appears at large length scales and not at short ones.

In order to address the question of the behavior below threshold, it is interesting to consider the small-temperature limit without, however, going all the way to  $T = 0$ , so that steady-state motion still exists. This limit is analogous to the  $T \rightarrow 0$  limit for the dynamics of a system at thermal equilibrium, where the Boltzmann weights impose a ground state occupation with probability 1. Occupation probabilities also exist for the steady-state dynamics in a finite system, but they are more difficult to compute. The  $T \rightarrow 0$  limit of this dynamical regime is thus described by a single dominant configuration, occupied with probability 1. This is particularly transparent for a particle hopping on a one-dimensional ring [22,23].

In this Letter, we construct this dominant configuration using a novel exact algorithm. We analyze its geometrical properties for driving forces between the equilibrium and the depinning threshold. We find, in agreement with the FRG scenario for  $f \ll f_c$ , that the depinning roughness exponent describes the geometry of the line at large length scales for all forces. This result is inconsistent with the existence of a divergent correlation length for  $f \rightarrow f_c^-$  in the steady-state regime. A divergent length scale exists only in the transient dynamics of relaxation to a metastable state. The conclusions of our analysis are summarized in the dynamical phase diagram of Fig. 1.

Let us consider an elastic line on a two-dimensional discrete  $L \times M$  lattice with periodic boundary conditions in both directions (see Fig. 2). The force  $f$  drives the line around the system in the direction of  $M$ . We define elementary moves as in Ref. [24], allowing for simultaneous motion of several sites. This avoids problems of single-site dynamics proper to the elastic string model. Using this dynamics, any configuration relaxes to the nearest metastable configuration, a local minimum of the energy

$$E = \sum_i \frac{1}{2} (h_{i+1} - h_i)^2 - fh_i + V(i, h_i). \quad (1)$$

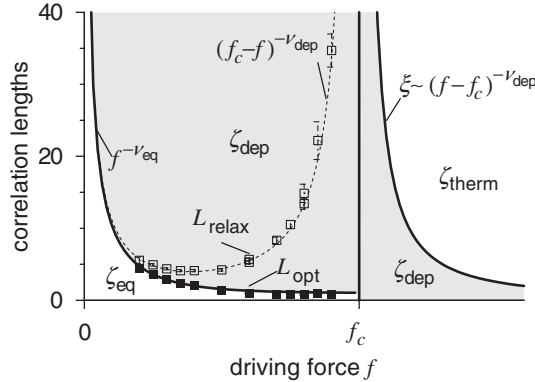


FIG. 1. Dynamical phase diagram. The steady-state properties of the elastic string at  $T \rightarrow 0$  are determined by  $L_{\text{opt}}$  (solid symbols) and  $\xi$ . They separate regions characterized by the equilibrium exponent, the depinning exponent (gray region), and the thermal one. The divergent length  $L_{\text{relax}}$  (open symbols) is associated only with transient dynamics. Lines are guides to the eye.

The first term in this equation takes into account the short-range elastic energy and  $V(i, h_i)$  is the quenched disorder, which we take to be Gaussian and uncorrelated. The variables  $h$  gives the height of the line, as a function of  $i$  (see Fig. 2). The equilibrium ground state (at  $f = 0$ ) is easily found with a transfer matrix approach [25]. The sample-dependent critical force  $f_c$  and the zero-temperature critical configuration at  $f_c$  are also readily determined [24] exploiting the analytic structure of the zero-temperature dynamics of a  $d$ -dimensional elastic interface embedded in a  $d + 1$  random medium. Two properties are particularly useful for numerical algorithms: the “no-passing” property assures that, during its motion, an elastic interface can never miss any pinned configuration; the “no-return” property, which holds after a finite initial time, states that only forward motion takes place [26]. At nonzero temperatures, these rules obviously cease to hold. The motion is dominated by the activation time spent to overcome the energy barriers. The evaluation of these barriers is an NP-complete problem [27] and the algorithms employed at the equilibrium are exponential in the size of the system. In the following we show that, in the  $T \rightarrow 0$  limit, properties analogous to the no-passing rule govern the time evolution of such systems. These properties allow one to capture the steady-state dynamics below the depinning threshold within a reasonable computation time.

For an elastic line pinned in a metastable configuration  $\alpha$ , the path taken at low temperature from  $\alpha$  to another metastable configuration with lower energy  $\gamma$  is the one with the lowest activation energy  $E_{\alpha}^{\text{esc}}$ . The time spent in  $\alpha$  thus corresponds to the Arrhenius activation energy  $E_{\alpha}^{\text{esc}}$ . Once at  $\gamma$ , the probability to return to  $\alpha$  is negligible if  $T \rightarrow 0$ . This procedure defines deterministic coarse-grained dynamics between metastable states. Two theorems can be proved for this dynamics, whenever the standard no-passing rule is valid: (i) If there is no configuration which lowers the energy of  $\alpha$  in the backward direction,

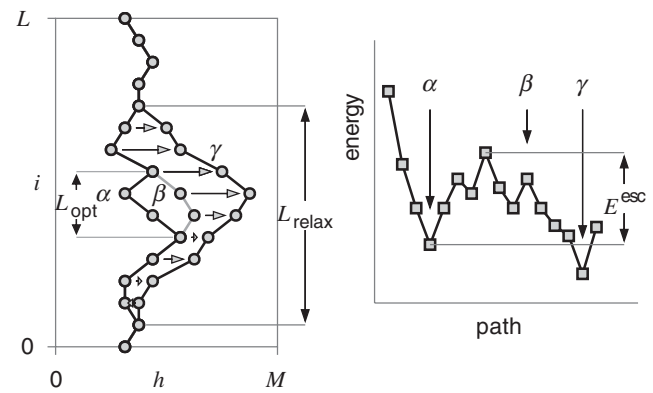


FIG. 2. Low-temperature dynamics of the driven elastic string below the depinning threshold: the optimal path to escape from a given metastable configuration  $\alpha$  pass through a saddle configuration  $\beta$  that can relax deterministically to the next metastable configuration  $\gamma$  with  $E_{\gamma} < E_{\alpha}$ . Configurations  $\alpha$  and  $\beta$  differ on a length  $L_{\text{opt}}$ ;  $\alpha$  and  $\gamma$  differ on a length  $L_{\text{relax}}$ .

the coarse-grained dynamics starting from  $\alpha$  is always forward directed. (ii) Let  $\alpha$  be any metastable configuration escaping into a configuration  $\gamma$  with  $h^\gamma \geq h^\alpha$ , and any  $\gamma'$  configuration such that  $h^{\gamma'} \geq h^\alpha$  and having an energy barrier  $E_{\gamma'}^{\text{esc}} > E_\alpha^{\text{esc}}$ : all  $\gamma'$  then satisfy  $h^{\gamma'} \geq h^\gamma$  [28]. Direct consequences of these theorems are that the dynamics is periodic after a single pass of the line around the system, and that the dominant configuration, the metastable configuration with the largest barrier, is always visited, independently of the initial condition. This dominant metastable configuration is the only statistically relevant configuration of the  $T \rightarrow 0$  steady-state dynamics: Under the conditions of Arrhenius activation, the system spends much more time in it than in any other configuration. To construct the minimal path escaping from the configuration  $\alpha$  (see Fig. 2), we enumerate all configurations dynamically connected to it, increasing gradually the maximum energy of configurations. This continues until a saddle configuration  $\beta$  is found which can relax to a metastable configuration  $\gamma$ , with  $E_\gamma < E_\alpha$ . Configurations  $\alpha$  and  $\beta$  differ on a length  $L_{\text{opt}}$ ;  $\alpha$  and  $\gamma$  differ on a length  $L_{\text{relax}}$ . A new path construction starts at configuration  $\gamma$ . Several refinements are implemented [28]. During the construction, a very large number of configurations are considered, but only those with energy barriers below  $E_\alpha^{\text{esc}}$  need to be evolved. In our case, the computational cost increases very rapidly with  $L_{\text{opt}}$ , but small values of  $L_{\text{opt}}$  can be handled even for large system sizes  $L$ . This is realized in the physically interesting case close to depinning, and the computation becomes difficult only for small driving forces, where the saddle point configuration may be very different from  $\alpha$ . We have considered systems up to  $L = 128$  for forces  $f \geq 0.7f_c$  and up to  $L = 32$  for  $f \sim 0.2f_c$ .

In the following, we concentrate on the disorder-averaged geometric properties of the dominant configuration, expressed through the structure factor  $S(q)$ , which gives access to the roughness exponent  $\zeta$ :

$$S(q) = \left| \sum_j h_j \exp(-iqj) \right|^2 \sim q^{-(1+2\zeta)}. \quad (2)$$

We also analyze the dynamical lengths  $L_{\text{opt}}$  and  $L_{\text{relax}}$  defined above. In Fig. 3(a), we show  $S(q)$  for different forces ranging from  $f = 0$  (equilibrium) to  $f = f_c$  (depinning). The slope of  $S(q)$  in these two limits corresponds to the critical exponents  $\zeta_{\text{eq}} = 2/3$  [29] and  $\zeta_{\text{dep}} = 1.26 \pm 0.01$  [12], respectively. In between, we find two regimes. Remarkably, on large length scales (small  $q$ ),  $S(q)$  corresponds to  $\zeta_{\text{dep}}$ , even at forces well below  $f_c$ . In Fig. 3(b) we show that this behavior is size independent up to  $L = 128$  at  $f = 0.8f_c$ . Only at small scales (large  $q$ ) is the roughness exponent  $\zeta_{\text{eq}}$ . This allows us to define a crossover length which decreases with increasing  $f$ , as we can see in Fig. 3(a). The results of Fig. 3 thus show that there is no divergent length scale below the depinning threshold in the steady-state regime, unlike the divergent length scale that exists above the threshold.

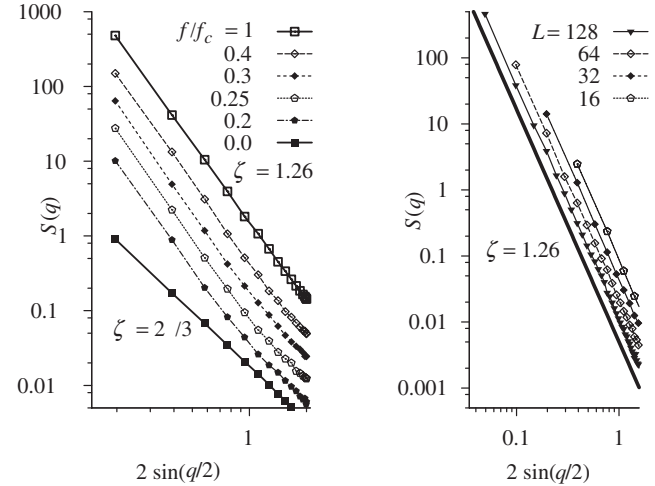


FIG. 3. Steady-state structure factor of the line in the  $T \rightarrow 0$  limit, averaged on 1000 samples. (a)  $S(q)$  for  $L = 32$ ,  $M = 92$ , and different forces (curves are shifted for clarity). (b)  $S(q)$  at  $f/f_c = 0.8$  for  $L = 16, 32, 64, 128$ , and  $M = L^{\zeta_{\text{dep}}}$ .

In order to understand the existence of a single characteristic length which does not diverge at  $f_c$  but separates the  $\zeta_{\text{eq}}$  and  $\zeta_{\text{dep}}$  steady-state regimes, we analyze the behavior of the dynamical lengths  $L_{\text{opt}}$  and  $L_{\text{relax}}$  as a function of  $f$ . The dynamical lengths shown in Fig. 1 are obtained starting from the dominant configuration and averaged on 1000 samples. We see that  $L_{\text{opt}}$  decreases with increasing  $f$  and saturates to the minimal avalanche size at  $f_c$ . Interestingly,  $L_{\text{relax}}$  increases as  $(f_c - f)^{-\nu_{\text{dep}}}$  close to  $f_c$  and  $L_{\text{relax}} \approx L_{\text{opt}}$  at low  $f$ . This behavior is controlled by the density of metastable states, which is very high at low forces and very low near  $f_c$ . The results of Fig. 1 lead us thus to identify  $L_{\text{opt}}$  with the steady-state crossover length. The observed divergence in  $L_{\text{relax}}$  has its origin purely in transient dynamics and has no counterpart in the steady-state properties. We note that  $L_{\text{relax}}$  can be related with the divergent length found in [15–17]. Our simulations lead to the dynamical phase diagram of Fig. 1. This diagram is expected to hold for  $d$ -dimensional manifolds in  $d + 1$  dimensions. The steady-state geometrical properties of the string in the  $T \rightarrow 0$  limit are determined by the two solid lines in Fig. 1:  $L_{\text{opt}}$ , associated with the optimal activated jump needed to escape from the dominant configuration, and  $\xi$ , the typical size of the depinning avalanche above threshold.  $L_{\text{opt}}(f)$  and  $\xi(f)$  separate three roughness regimes:  $\zeta_{\text{eq}} = 2/3$ ,  $\zeta_{\text{dep}} = 1.26$ , and  $\zeta_{\text{therm}} = 0.5$ . The divergent length  $L_{\text{relax}}$  (dashed line) does not affect steady-state properties: it describes transient processes that depend on the distance between successive metastable states, but it does not describe the properties of the dominant ones. As indicated in Fig. 1, it is plausible to connect continuously  $L_{\text{opt}}$  with the thermal nucleus size  $\xi_T$  defined for  $f \ll f_c$ . However, we are not able to verify with our data the predicted power law divergence  $\xi_T \sim f^{-\nu_{\text{eq}}}$ . The scenario thus proposed is consistent with the

FRG prediction [20] of the existence of  $\zeta_{\text{dep}}$  at scales larger than  $\xi_T$  and inconsistent with the existence of a critical region extending both below and above  $f_c$ , as the standard critical phenomena interpretation would have suggested.

An interesting question is whether the elastic depinning has a counterpart in a static although nonstandard type of phase transition. Both pure and disordered systems can exhibit a critical low-temperature phase at equilibrium, such as the XY and the 2D random-phase sine-Gordon [30] models. However, the latter examples display a line of critical points and temperature-dependent exponents, while for  $f < f_c$  the roughness exponent of the string is force independent. In order to get parameter independent exponents, one usually needs the existence of an extra symmetry, as in the Kondo problem [31]. Whether an analogous counterpart exists for the string is yet unclear, though. Critical nonequilibrium phases are, on the other hand, a common (although less understood) phenomena. In this respect, let us note that depinning at  $T = 0$  is an absorbing phase transition [32]. From this general viewpoint the  $T \rightarrow 0$  creep dynamics for  $0 < f < f_c$  can be thought as an effective feedback mechanism that keeps a critical “activity” in the system above the length scale  $L_{\text{opt}}$  [20,21]. Understanding the links of the depinning transition with other static or dynamic phase transitions is thus a very appealing challenge.

Although our computational approach strictly holds only in the  $T \rightarrow 0$  limit, it yields the scenario of Fig. 1, which offers a solid framework for discussing finite temperature effects. At finite temperature the depinning transition is rounded. Since the velocity is finite for all forces, the regime with the thermal roughness  $\zeta_{\text{therm}}$  exists at the largest length scales [20]. For  $f < f_c$  we expect two crossovers separating the regimes  $\zeta_{\text{eq}}$ ,  $\zeta_{\text{dep}}$ , and  $\zeta_{\text{therm}}$ , as we increase the length scale. For temperature comparable to the strength of the disorder at the very small length scales an additional thermal regime appears and crosses over to  $\zeta_{\text{eq}}$  or directly to  $\zeta_{\text{dep}}$ . Such a scenario is in part supported by recent Langevin dynamics simulations [21], which show, at small forces, a steady-state motion characterized by a roughness exponent bigger than  $\zeta_{\text{eq}}$  at large length scales and a roughness  $\zeta_{\text{therm}}$  at the smallest length scales.

Finally, we expect that an experimental verification of our results is possible using, for instance, imaging techniques for magnetic [3,4] or electric [5,6] domain walls in thin films:  $L_{\text{opt}}$  could be extracted from the analysis of a spatial correlation function or by measuring the domain wall speed at low temperatures, since  $L_{\text{opt}}$  also controls the thermally activated motion [28];  $L_{\text{relax}}$  could be measured by comparing consecutive (long-lived) metastable states when  $f$  is close to  $f_c$ , since then  $L_{\text{relax}}$  controls the distances between successive metastable states.

We thank P. Le Doussal for very helpful discussions all along this work and also acknowledge stimulating discussions with C. J. Bolech and A. A. Middleton. We are grate-

ful to J. Albiero for useful programming advice. A. R. and W. K. thank DPMC in Geneva for hospitality during part of this work. This work was supported in part by the Swiss National Fund under MANEP and Division II.

- 
- [1] D. T. Fuchs *et al.*, Phys. Rev. Lett. **80**, 4971 (1998).
  - [2] S. G. Lemay *et al.*, Phys. Rev. Lett. **83**, 2793 (1999).
  - [3] S. Lemerle *et al.*, Phys. Rev. Lett. **80**, 849 (1998).
  - [4] V. Repain *et al.*, Europhys. Lett. **68**, 460 (2004).
  - [5] T. Tybell *et al.*, Phys. Rev. Lett. **89**, 097601 (2002).
  - [6] P. Paruch, T. Giamarchi, and J. M. Triscone, Phys. Rev. Lett. **94**, 197601 (2005).
  - [7] S. Moulinet *et al.*, Phys. Rev. E **69**, 035103(R) (2004).
  - [8] L. Ponson, D. Bonamy, and E. Bouchaud, Phys. Rev. Lett. **96**, 035506 (2006); K. J. Måløy and J. Schmittbuhl, Phys. Rev. Lett. **87**, 105502 (2001).
  - [9] O. Narayan and D. S. Fisher, Phys. Rev. B **46**, 11520 (1992).
  - [10] T. Nattermann, S. Stepanow, L. H. Tang, and H. Leschhorn, J. Phys. (Paris) **2**, 1483 (1992).
  - [11] P. Chauve, P. Le Doussal, and K. Wiese, Phys. Rev. Lett. **86**, 1785 (2001).
  - [12] A. Rosso, A. K. Hartmann, and W. Krauth, Phys. Rev. E **67**, 021602 (2003).
  - [13] O. Duemmer and W. Krauth, Phys. Rev. E **71**, 061601 (2005).
  - [14] D. S. Fisher, Phys. Rev. B **31**, 1396 (1985).
  - [15] A. A. Middleton and D. S. Fisher, Phys. Rev. B **47**, 3530 (1993).
  - [16] O. Narayan and A. A. Middleton, Phys. Rev. B **49**, 244 (1994).
  - [17] L. W. Chen and M. C. Marchetti, Phys. Rev. B **51**, 6296 (1995).
  - [18] L. B. Ioffe and V. M. Vinokur, J. Phys. C **20**, 6149 (1987).
  - [19] T. Nattermann, Europhys. Lett. **4**, 1241 (1987).
  - [20] P. Chauve, T. Giamarchi, and P. Le Doussal, Phys. Rev. B **62**, 6241 (2000).
  - [21] A. B. Kolton, A. Rosso, and T. Giamarchi, Phys. Rev. Lett. **94**, 047002 (2005).
  - [22] B. Derrida, J. Stat. Phys. **31**, 433 (1983).
  - [23] P. Le Doussal and V. M. Vinokur, Physica (Amsterdam) **254C**, 63 (1995); P. Le Doussal (private communication).
  - [24] A. Rosso and W. Krauth, Phys. Rev. B **65**, 012202 (2001); Phys. Rev. Lett. **87**, 187002 (2001).
  - [25] D. A. Huse and C. L. Henley, Phys. Rev. Lett. **54**, 2708 (1985); M. Kardar, Phys. Rev. Lett. **55**, 2923 (1985).
  - [26] A. A. Middleton, Phys. Rev. Lett. **68**, 670 (1992).
  - [27] A. A. Middleton, Phys. Rev. E **59**, 2571 (1999).
  - [28] A. B. Kolton, A. Rosso, T. Giamarchi, and W. Krauth (to be published).
  - [29] M. Kardar, Nucl. Phys. **B290**, 582 (1987).
  - [30] J. L. Cardy and S. Ostlund, Phys. Rev. B **25**, 6899 (1982).
  - [31] K. G. Wilson, Rev. Mod. Phys. **47**, 773 (1975).
  - [32] J. Marro and R. Dickman, *Nonequilibrium Phase Transitions in Lattice Models* (Cambridge University Press, Cambridge, 1990); H. Hinrichsen, Adv. Phys. **49**, 815 (2000); G. Odor, Rev. Mod. Phys. **76**, 663 (2004).